2018-07-01

Strontium Isotopes-A Tracer for Dust and Flow Processes in an Alpine Catchment

Colin Andrus Hale
Brigham Young University

Strontium Isotopes – A Tracer for Dust and Flow Processes in an Alpine Catchment

Colin Andrus Hale

A thesis submitted to the faculty of
Brigham Young University
in partial fulfillment of the requirements for the degree of

Master of Science

Gregory T. Carling, Chair
Stephen T. Nelson
Zachary T. Aanderud
Paul D. Brooks

Department of Geological Sciences

Brigham Young University

ABSTRACT

Strontium Isotopes – A Tracer for Dust and Flow Processes
in an Alpine Catchment

Colin Andrus Hale
Department of Geological Sciences, BYU
Master of Science

Stream chemistry changes in response to snowmelt, but does not typically reflect the chemistry of the snowpack. This suggests that flow processes between snowmelt and stream system, such as interactions with the soil and bedrock, have an important control on water chemistry and highlight the complex flow pathways from the snowpack to stream. To investigate flow processes in the upper Provo River watershed, northern Utah, we sampled three sites on the river ~20 times per year during 2016 and 2017. The sites, from highest elevations to lowest were Soapstone, Woodland, and Hailstone, corresponding to locations of active stream gauges. To identify possible water sources to the stream during snowmelt, water samples were taken for snow, ephemeral streams, soil water, lake, and spring water. To investigate potential impacts of mineralogy, samples were taken for dust, soil and bedrock. The upper Provo River showed distinct temporal variation in filtered (<0.45 microns) stream water for $^{87}Sr/^{86}Sr$, dissolved organic carbon (DOC), silica (Si), and Lead (Pb) during the snowmelt season. The watershed has distinct $^{87}Sr/^{86}Sr$ ratios for bedrock (0.7449 ± 0.0208), soil (0.7131 ± 0.0010) , and dust (0.7106 ± 0.00044). Differences in chemical signatures allows for interpretations between shallow flowpaths and intermediate flowpaths, where shallow flowpaths react primarily with soil, and intermediate flowpaths that react mainly with the bedrock. The $^{87}Sr/^{86}Sr$ ratio at the highest elevation site (Soapstone) was significantly different during the snowmelt season (March-August) relative to the rest of the year, with averages of 0.7155 ± 0.0011 and 0.7165 ± 0.0007, respectively. A four-component (shallow flowpath, intermediate flowpath, base flow, and snow) mixing model utilizing Sr concentrations and $^{87}Sr/^{86}Sr$ ratios showed shallow and intermediate flowpaths were the dominant controls of stream chemistry during snowmelt. These results were supported by a 24-hour sampling event where DOC, Si, and Pb showed clockwise hysteresis patterns during snowmelt. This hysteresis pattern suggests that changes in stream chemistry are sourced from changes in stream discharge related to shallow flowpaths fed by snowmelt. The chemical signature of the shallow flowpath is associated with the accumulation of dust in the soil profile. This dust signature has significant impact on stream chemistry for heavy metals and REE concentrations. This signature is propagated downstream through the nested catchment suggesting that processes at meltwater sources have significant impacts on water chemistry through the entire catchment. Distinct $^{87}Sr/^{86}Sr$ ratios and REE patterns were observed for 2016 and 2017 at the lower sites (Woodland and Hailstone), suggesting that climate may play a role in stream chemistry during the snowmelt season. These findings indicate that climate and dust deposition can have significant impacts on water quality in an alpine catchment.

Key Words: Strontium Isotopes, $^{87}Sr/^{86}Sr$, Trace metals, DOC, Flowpaths, Residence Time, Dust, Nested Catchment

ACKNOWLEDGMENTS

Firstly, I would like to thank my advisor Dr. Gregory Carling for his guidance and support through my undergraduate and graduate degrees. I would also like to give special thanks to each of my thesis committee members, Dr. Stephen Nelson, Dr. Zachary Aanderud, and Dr. Paul Brooks for their insights and direction in furthering my research. Special thanks to Dr. Diego Fernandez at the University Utah for assistance in laboratory analysis for cations and elements isotopes. Lastly, I would like to thank Brian Packer, and Hannah Checketts fellow graduate students who worked on this same study with me.

TABLE OF CONTENTS

LIST OF FIGURES

1. Introduction

During meltwater events in alpine catchments, changes in stream chemistry during the increased discharge reflect inputs from various water sources including soil water, groundwater, and precipitation. While it is expected that the increased discharge is sourced from event water (snowmelt or rain), chemical signatures in streams indicate that the water is actually derived from rapidly released pre-event water that is stored in the catchment (Kirchner, 2003; McNamara et al., 2011). With this conceptual underpinning, flow models typically rely on soil water to account for increased stream discharge during precipitation or snowmelt events (Burns et al/, 2001; Liu et al., 2008). However, typical alpine catchments lack sufficient soil water to account for the increased discharge even though soil water can have a major impact on stream chemistry (Liu et al., 2004; Foks et al., 2018). Therefore, new conceptual models are needed to explain both the increased discharge during meltwater events and the changes in stream chemistry without relying solely on the idea of rapidly-released soil storage water. This new conceptual model for alpine catchments would help to "get the right answer for the right reasons" (Kirchner, 2006). In this paper, we describe a new conceptual model for meltwater flowpaths that influence stream chemistry and discharge relying on water chemistry to interpret flowpath depths as a function of reaction paths and residence times.

Many alpine catchments in the Rocky Mountains are influenced by atmospheric dust deposition (Reynolds et al., 2003; Reynolds et al., 2010). Dust deposition in these catchments may play a major role in stream chemistry (Vázquez-Ortega et al., 2015). Dust in soil may

become more important as dust deposition increase in the western US (Neff et al., 2008). In addition, dust deposition within western US snowpack is adding additional solutes to the meltwater (Clow et al., 2016; Carling et al., 2012). Dust in soil may have greater impact water chemistry, since stream chemistry is sensitive to climate conditions and influenced heavily by soil signatures in the Rocky Mountains (Foks et al., 2018). Thus, it is important to understand the role that dust deposition may have on water quality during snowmelt.

Concentration-discharge (C-Q) relationships can describe solute availability and sources within a watershed (Godsey et al., 2009). Utilizing these C-Q relationship inferences can be made about water sources and flowpaths (Kim et al., 2017; Godsey et al., 2009). For example, a positive slope for a hysteresis loop could be ascribed to a flushing effect. Alternatively, a negative slope in a hysteresis loop suggests a dilution effect (Godsey et al., 2009). There is also a lack of understanding with nested catchment, and how these relationships change with distance and scale in the catchment.

Strontium isotope ratios ($^{87}Sr/^{86}Sr$) are an effective tracer for investigating flowpaths in alpine catchments. The $^{87}Sr/^{86}Sr$ ratio does not fractionate significantly in nature, making it an ideal tracer for investigating solute sources from chemical or biological weathering from natural variations of $^{87}Sr/^{86}Sr$ ratios in sources (Hogan et al., 2003). ^{86}Sr is a nonradiogenic isotope, whereas ^{87}Sr is produced from the decay of ^{87}Rb. ^{87}Rb has a half-life of 4.8×10^{10} years, thus making the ratios stable for the duration of this study. A limited number of studies have utilized $^{87}Sr/^{86}Sr$ ratio as a tracer in catchment hydrology (Hogan et al., 2003; Andrews et al., 2016). This underutilized tool can be especially useful in distinguishing soil signatures from bedrock

signatures where atmospheric dust $^{87}Sr/^{86}Sr$ ratios are significantly different from bedrock (Hogan et al., 2003). This tool can be especially useful in catchments where the $^{87}Sr/^{86}Sr$ ratio in dust is significantly different than bedrock (Munroe, in prep;).

The purpose of this study is to identify water flowpaths during snowmelt in the upper Provo River, an alpine headwater stream in the Uinta Mountains, Utah, USA. Our three main objectives are to: (1) Determine solute sources to the stream during snowmelt, (2) Compare relative contribution of sources to the stream during snowmelt, and (3) compare similarities or differences in stream chemistry for a nested catchment. The upper Provo River watershed was chosen because soil is heavily influenced by atmospheric dust, making the chemical soil signature and $^{87}Sr/^{86}Sr$ ratio significantly different from bedrock. In addition, the upper Provo River watershed contains several monitoring stations. The United States Geological Survey (USGS) has stream gauges at Hailstone and Woodland that monitor discharge at 15-min intervals. Further, aquatic monitoring stations were installed at Soapstone and Woodland as part of the iUTAH project, funded by the National Science Foundation EPSCoR program. These aquatic sites monitor temperature, specific conductance, pH, dissolved oxygen, turbidity, colored dissolved organic matter, and discharge (at Soapstone). There are also two SNOTEL (snow telemetry) sites in the watershed monitoring precipitation, snowpack depth, snowpack water content, and temperature.

2. Methods

2.1 Study Area

The upper Provo River watershed is an ideal location to investigate flowpath processes during snowmelt. The watershed is located in northern Utah, USA, in the south-eastern portion of the Uinta Mountain Range and covers 675 km^2 (Fig. 1). The upper watershed is primarily vegetated by lodgepole pine and douglas fir (Lowry et al., 2005). The lower portion of the watershed is primarily vegetated by sedge and sage brush with minor agricultural activity. The headwaters of the upper Provo River start in the subalpine zone of the Uinta Mountains (3060 m asl) and end at Jordanelle Reservoir (1880 m asl) running a total length of 50 km. The stream receives diverted water from the Duchesne River watershed (104 km^2) and the Weber River watershed (589 km^2). The Duchesne diversion is above the Soapstone sampling site, and the Weber River diversion is between the Woodland and Hailstone sampling sites (Fig. 1).

Sampling sites were chosen based on distinctions between geological settings. Above the upper site, Soapstone, the bedrock is primarily composed of interbedded metasedimentary units overlain by quaternary glacial deposits and aeolian dust deposition. The aeolian dust deposition is essential to use $^{87}Sr/^{86}Sr$ ratios to differentiate between shallow flowpaths in the soil and deep flowpaths in the bedrock. The geological setting from the diverted watersheds is similar to Soapstone. At the Woodland site, the bedrock is primarily composed of Paleozoic carbonate and other sedimentary rocks. At the lower site, Hailstone, the bedrock is primarily composed of Tertiary volcanic rocks.

2.2 Sample Collection and Preparation

To identify changes in stream chemistry and potential water sources, stream water, ephemeral streams, soil water, springs, lakes, snow, soil and dust were sampled in the upper Provo River watershed from 2013-2017. The upper Provo River was sampled at Soapstone (n=87), Woodland (n=46) and Hailstone (n=52) (Fig 1). Samples were taken throughout the water year with sampling frequency increased during the snowmelt season. Ephemeral streams (n=17), which are seasonal snowmelt rivulets that chemically mix with underlying soil were sampled during the 2016 and 2017 water years. Soil water (n=2) was sampled during the 2017 water year to compare with ephemeral stream samples. Springs (n=6) were sampled simultaneously with ephemeral streams during the 2016-2017 water years. Lake (n=3) were sampled during 2013 water year. Snow sampling (n=72) was conducted from 2013-2017.

To avoid confusion with other terminology, this study uses the term ephemeral streams or shallow flowpaths to describe event water that is reacting with the soil, and could be considered "event soil water". Ephemeral streams are seasonal snowmelt channels that develop during spring runoff. This study relies on the ephemeral stream signature to indicate importance of soil impact on stream chemistry during snowmelt. Two soil water samples were taken to compare with ephemeral stream signature. In this paper, we use water chemistry to interpret flowpath depths as a function of reaction paths and residence times. For example, we assume that water primarily traveling through shallow flowpaths react with the soil, have a short flowpaths and short residence times. Likewise, water that primarily travels through deep flowpaths would react

with bedrock, have a long flowpath lengths and long residence times. Using this assumption, we can investigate stream water contribution by linking chemical signatures to flowpaths.

All water samples (stream, ephemeral, soil water, springs and lakes) were collected using the EPA "clean hands, dirty hands" method (USEPA, 1996). All DOC samples were filtered using a 0.45-micron fiberglass disk filter, and trace metal samples were filtered with clean 0.45-micron PES syringe filters. LDPE bottles were used for major and trace elements, including Sr isotopes. Separate amber glass bottles were used for water isotopes and DOC. Prior to sampling, LDPE bottles were 24-hour acid washed with 10% v/v HCL, then triple rinsed with Milli-Q water, and stored in clean Ziploc bags. Amber vials were rinsed with 10% v/v HCL, triple rinsed with Milli-Q water, then baked in an oven for at least 3 hours at 450 degrees C and covered with aluminum foil that was also in the same oven. Both Trace metal and elemental isotope samples are preserved with 2.4% v/v TMG HNO3. DOC samples are preserved by acidifying to a pH of 2-3 with TMG HCL. After filtering and acidifying, individual samples are stored at 4°C until analysis. Field blanks were taken at each site by pouring Milli-Q water into sample bottles, then following the same sample preparation for the type of sample.

Snow samples were taken to identify snowpack contribution to stream chemistry during snowmelt. Snow sampling followed procedures in accordance to Carling et al. (2012) by digging three snow pits at each site within 10 cm of the ground. Multiple snow pits are sampled at each location to mitigate sampling error and irregularities. Temperature and visual observations of each snow pit were taken in 10 cm increments. Acid washed acrylic tubes measuring 45.5cm x 5.5 cm were used to collect snow cores. Snow cores were transferred into triple rinsed clean 2.5 L FLPE bottles and then double bagged. All snow samples were collected in accordance to

"clean hands, dirty hands" method established by the EPA to prevent contamination (USEPA, 1996). A field blank of Milli-Q water was taken at each site as a control by pouring water through acrylic tubes into sampling bottle. After collection, the snow samples were then transported on ice and stored at below freezing temperatures until subsampling occurred. During subsampling the bottles containing snow are removed from storage bags. The bottle surface is triple rinsed in Milli-Q water. Bottles are then placed in laminar flow and allowed to thaw. Just prior to melt, the snow is fractioned into different subsample bottles then followed the same methods as water samples. Dust samples were also taken at snow pit sites by scraping dust layers into clean 2 liter LDPE bottles. The samples were melted in laminar flow hood and excess water was poured off. Dust samples were then dried and followed same steps as soil sediment leaches (described below).

To investigate contribution from the soil to stream chemistry during snowmelt, soil pits were excavated to bedrock in two locations above the Soapstone sampling site. Soil pit depths were 40 cm and 50 cm. Samples were taken in 10 cm increments with a clean plastic tool, and stored in clean Ziploc bags. Samples were stored at 4 C until analysis preparation. Samples were dried in a laminar flow hood, then approximately 200 micrograms were split for sequential leaching with an ammonium acetate buffer at 7 pH, 1M acetic acid, 1M nitric acid, and aqua regia. Samples were leached for 24 hours by each leachate, and rinsed in Milli-Q water before the following leach step. Leachates were analyzed using the same method at trace elements and for water samples.

2.3 Sample Analysis

To identify stream chemistry and potential sources, samples were analyzed for trace element and major cation concentrations using an Agilent 7500ce quadrupole inductively coupled plasma mass spectrometer (ICP-MS) with a collision cell, a double-pass spray chamber with perfluoroalkoxy (PFA) nebulizer (0.1 mL/min), a quartz torch, and platinum cones. Concentrations were measured for the following 40 elements: Ag, Al, As, B, Ba, Be, Ca, Cd, Ce, Co, Cr, Cs, Cu, Dy, Er, Eu Fe, Gd, Ho, K, La, Li, Lu, Mg, Mn, Mo, Na, Nd, Ni, Pb, Pr, Rb, Sb, Sc, Se, Sm, Sr, Tb, Th, Ti, Tl, U, V, Y, Yb, and Zn. Al, Ca, Cr, Fe, K, Mn, Na, and V were determined using 4 mL He/min in the collision cell, As and Se were determined using 4 mL He/min plus 2.5 mL H2/min, and the other 30 elements were determined using Ar as the carrier gas. DL was determined as three times the standard deviation of all blanks analyzed throughout each run. A NIST standard reference material (SRM 1643e) were analyzed multiple times in each run together with the samples as a continuing calibration verification. The long-term reproducibility and SRM 1643e show that our results are consistently accurate within 10% for most elements. DOC samples were analyzed by total organic carbon isotope radio mass spectrometry (TOC-IRMS).

To identify stream chemistry and potential sources and flowpaths, a subset of samples were analyzed for $^{87}Sr/^{86}Sr$ ratios using a Thermo Scientific Neptune multicollector ICP-MS. The samples were purified inline using a Sr-FAST ion chromatographic column packed with a crown ether resin. Analytical precision (2σSE) of all samples ranged from ±00001 – 0012. The $^{87}Sr/^{86}Sr$ ratios were corrected for mass bias using an exponential law, normalizing to $^{86}Sr/^{88}Sr$ =

0.1194 (Steiger and Jäger, 1977). Isobaric interferences on the $^{87}Sr/^{86}Sr$ ratios, such as from ^{87}Rb and ^{86}Kr, were corrected by simultaneous monitoring of ^{85}Rb and ^{83}Kr using the corresponding invariant ratios of $^{87}Rb/^{85}Rb = 0.385706$ and $^{86}Kr/^{83}Kr = 1.502522$ (Steiger and Jäger, 1977).

2.4 Analytical Techniques

To identify water contributions from different sources in the upper watershed, we developed mixing models using end-member chemistry from snow, groundwater, and other potential sources. Statistical analysis and mixing models were completed in MATLAB. $^{87}Sr/^{86}Sr$ mixing uses the same equation used in Clark and Fitz (1997). The mixing line between two end-members' equation is the below equation. This mixing equation cannot explain mixing between four sources.

$$Sr\ ratio\ mix = \frac{(Sr_2 * Sr_2)(^{87}_{86}Sr_2 - ^{87}_{86}Sr_1)}{Sr_1(Sr_1 - Sr_2)} + \frac{(Sr * ^{87}_{86}Sr_1) - S_2 * ^{87}_{86}Sr_2}{Sr_1 - Sr_2}$$

Where, Sr_1 and Sr_1 are Sr concentrations for end-members, $^{87}_{86}Sr_1$ and $^{87}_{86}Sr_2$ are $^{87}Sr/^{86}Sr$ ratios for end-members, and Sr is an array where $Sr = (Sr_1 * F) + (Sr_2(1 - F))$, where F is an array of fraction percentages from 0-1. This same method is applied to each endmember set to generate mixing lines.

To compare statistical differences between sources and seasonal stream differences for $^{87}Sr/^{86}Sr$ a one-way analysis of variance was used. This one-way analysis of variance compares the 95% confidence interval about the mean to other groups. This analysis assumes groups are sampled from a normal distribution.

3. Results

3.1 Strontium and stream response to spring runoff

Strontium (Sr) concentrations and $^{87}Sr/^{86}Sr$ ratios varied with stream discharge in the Provo River (Fig. 2). At the upper site (Soapstone), during 2014-2017 peak discharge occurred during the months of May or June with the lowest discharge in 2015 (27.6 m^3/s) and highest discharge in 2017 (50.38 m^3/s), compared with typical base flow discharge below 0.5 m^3/s. Sr concentrations were consistently around 17 ppb through base flow and snowmelt. $^{87}Sr/^{86}Sr$ ratios decreased from a maximum of 0.7172 during base flow to a minimum of 0.7130 during snowmelt. $^{87}Sr/^{86}Sr$ ranged from 0.7169 and 0.7130 during spring runoff, and averaged at 0.7155 $\pm$ 0.0011. The $^{87}Sr/^{86}Sr$ ratio ranged from 0.7172 to 0.7153 during base flow and averaged at 0.7165 $\pm$ 0.0007.

At Woodland and Hailstone, Sr concentrations decreased, while the $^{87}Sr/^{86}Sr$ ratio increased in response to spring runoff (Fig. 2). Peak discharge during the 2014-2017 study period occurred during the months of May or June with the lowest peak discharge in 2015 (34.0 and 54.0 m^3/s) and highest peak discharge in 2017 (71.4 and 90.0 m^3/s), compared with typical base flow discharge around 2 m^3/s and 3 m^3/s respectively. The $^{87}Sr/^{86}Sr$ ratio averaged at 0.7096 $\pm$ 0.0002 and 0.70980 $\pm$ 0.0001 during base flow and decreased to a minimum of 0.7079 and 0.7099, respectively, during peak discharge.

3.2 Sr isotopes in different water sources and geologic media

Stream water and catchment water sources showed a wide range of $^{87}Sr/^{86}Sr$ ratios from 0.7737 in bedrock (Monroe, personal communication) to 0.7100 from dust in snow in the upper Provo River watershed (Fig. 3). A one-way analysis of variance showed statistical difference between dust, soil and bedrock for $^{87}Sr/^{86}Sr$ measurements. The $^{87}Sr/^{86}Sr$ ratio from the water sources snow, ephemeral streams, lake and springs are 0.7106 ± 0.0004, 0.7131 ± 0.0010, 0.7129 ± 0.0012, and 0.7178 ± 0.0024 respectively. During base flow the mean $^{87}Sr/^{86}Sr$ ratio for Soapstone, Woodland and Hailstone is 0.7165 ± 0.0007, 0.7096 ± 0.0002, and 0.7098 ± 0.00015, compared to the mean $^{87}Sr/^{86}Sr$ ratio during spring runoff which is 0.7155 ± 0.0011, 0.7110 ± 0.0006, and 0.7110 ± 0.0005. A two-sample t-test comparing high flow and base flow $^{87}Sr/^{86}Sr$ ratio at the same site showed that samples were statistically different with p values of 0.0051 for Soapstone, 0.000002 for Woodland and for 0.000002 Hailstone.

3.3 Concentration discharge relationships show increasing and decreasing relationships

Concentration-discharge relationships reveal different patterns for specific elements which can help interpret flow mechanisms and pathways. At the upper site (Soapstone), the $^{87}Sr/^{86}Sr$ ratio decreased with discharge, while DOC and Pb concentrations increased with discharge and Si concentrations showed chemostatic behavior (Fig. 4). All hysteresis loops were clockwise at Soapstone. Not shown are other elements trace elements that showed a similar pattern as Pb but with slightly more elevated concentrations directly after initial increase in discharge. Hourly samples were taken for 24-hours. These samples show a clockwise daily

hysteresis for DOC, Si, and Pb. Woodland and Hailstone show similar patterns in concentration discharge plots. $^{87}Sr/^{86}Sr$ ratios were elevated at both sites with discharge. Also, $^{87}Sr/^{86}Sr$ ratios for 2017 showed a different trend than for 2014-2016. DOC and Pb showed elevated concentrations with discharge, and Si showed a dilution trend with discharge. DOC, Si, and Pb showed clockwise hysteresis patterns, while some elements not shown had figure eight or counter-clock-wise hysteresis loops.

4. Discussion

4.1 Upper Provo River solute sources

Soil water is the primary source of solutes to the upper Provo River watershed during the snowmelt season. The stream system receives the majority of solutes derived from bedrock, soil and dust in snow that is contained in the soil. The upper portion of the watershed is primarily composed of quartzite bedrock (Fig. 1). Quartzite is primarily made of silica and offers little contribution of Sr, DOC, and Pb (Reynolds 2010). In contrast, Uinta Mountain soils are heavily influenced by atmospheric dust with elevated concentrations of Sr, Pb, and other trace elements relative to local bedrock. In addition, atmospheric dust has significantly lower $^{87}Sr/^{86}Sr$ ratios than bedrock (Fig. 3). The Uinta snowpack is also influenced by similar dust deposition, however, solute concentrations in snow are too low to attribute changes in stream chemistry during snowmelt for Sr, and other elements (Figs. 2, 3, 4). Previous studies have shown that dust can be a significant contributor of solutes to stream systems (Vázquez-Ortega et al, 2015). Dust

may become especially important for soil over quartzite, where dust deposition may contribute up to 90-100% of nutrient solutes (Miller et al., 2014).

Biological activity and other processes in in the soil profile may increase chemical impact from soil. Elevated concentrations of DOC during snowmelt can be explained from meltwater rapidly accumulating DOC from soil (Bishop et al., 2004). Si concentrations in the stream are typically used to infer source water residence times. However, biological activity in the soil profile can increase organic acids releasing Si and other elements causing elevated concentrations in the stream (Amundun et al, 2007; Amelia et al., 2017). Elevated concentrations of REE in stream may be attributed to complexation of DOM in the soil, suggesting that biological activity may mediate REE chemical denudation from soil to solution (Vázquez-Ortega et al, 2015). Further study is needed to determine the importance of biological activity and its relationship to stream chemistry. Especially with work in the Rocky Mountains showing that stream chemistry is sensitive to climate changes (Foks et al., 2018), are these relationships may be influence by biological activity.

4.2 Relative contribution of water with short and intermediate flow depths during runoff at up-stream site

To investigate changes in stream sources during snowmelt, a four-component mixing model utilizing Sr concentrations and $^{87}Sr/^{86}Sr$ ratios was constructed (Figure 6). End-members for mixing model are shallow flowpaths, intermediate flowpaths, base flow and snow. Shallow flowpaths were used to identify the contribution from soil. The shallow flowpath end-member was constrained by sampling ephemeral streams and soil water. Intermediate flowpaths signature

was measured by sampling various spring systems above Soapstone. Base flow is a mixture of deeper flowpaths and lake water. We assumed that base flow chemical signature is consistent through the year. Using this assumption, we constrained base flow signature end-member by stream samples at Soapstone during September-February. Snow chemical signature was constrained by bulk snowpack samples. A two-component mixing model between any viable of the sources does not account for the variance in Sr concentrations and $^{87}Sr/^{86}Sr$ ratios. A three-component mixing model with shallow flowpath, base flow and snow can account for all variations in Sr concentration and $^{87}Sr/^{86}Sr$ ratios during snowmelt, however, the stream signature trend after peak discharge followed closely to a mixing line between shallow flowpath and intermediate flowpath signatures. This trend suggests that stream water during snowmelt can be explained well by mixing between shallow flowpath and intermediate flowpath water.

Mixing model end-members were constructed to be conservative for shallow flowpaths, intermediate flowpath, and base flow to avoid over-estimating a source (Fig. 5). Shallow flowpath end-member was the maximum Sr concentration and minimum $^{87}Sr/^{86}Sr$ ratio for soil water and ephemeral stream samples. The intermediate flowpath end-member was the minimum Sr concentration and maximum $^{87}Sr/^{86}Sr$ ratio for spring samples. Base flow was chosen as the maximum Sr concentration and $^{87}Sr/^{86}Sr$ ratio during base flow. The snow end-member was the average Sr concentration and $^{87}Sr/^{86}Sr$ ratio for snow samples (Fig. 5).

The mixing analysis using Sr concentration and $^{87}Sr/^{86}Sr$ ratios indicates that shallow flowpaths and intermediate flowpaths are the dominate source contributions during spring runoff (Fig. 6). During the rising limb of the hydrograph, the Sr concentrations and $^{87}Sr/^{86}Sr$ ratios trend toward the shallow flowpath signature. After peak discharge the signature shifts towards

intermediate flowpath signature, then gradually returns to base flow signature. This indicates that shallow and intermediate flowpaths are the predominate transport mechanisms for water to the stream system. The change in Sr concentration and $^{87}Sr/^{86}Sr$ ratio can also be interpreted as a mixing between snowmelt and base flow. This may be explained by higher elevation snowmelt with less soil to react with before reaching the stream or a flushing of available solutes from the soil system by initial melt waters. These both seem improbable because waters from higher elevations will have longer travel times so have more time to react and soil leaching showed high concentrations of exchangeable solutes still available. In addition, the delay in time for intermediate flowpaths match well with increased residence time due to deeper and longer flowpaths.

C-Q relationships for DOC, Si, and Pb support end-member mixing analysis that shallow flowpaths and intermediate flowpaths are a major contribution to stream chemistry during snowmelt. C-Q patterns for DOC, Si and Pb all show clockwise hysteresis loops, on both a yearly and daily cycle (Fig 4). The yearly clockwise hysteresis is generally attributed to a "flushing" effect on the soil profile (Godsey et al., 2009). However, this same pattern can also be explained by changes in water sources during the precipitation or snowmelt events. This second theory is also supported by the daily hysteresis pattern for DOC, Si, and Pb during snowmelt, and the yearly $^{87}Sr/^{86}Sr$ ratio hysteresis pattern (Fig. 4). The daily hysteresis cycle can be attributed to the daily changes influx of snowmelt during the day. This influx increases the discharge in the stream from the shallow flowpath ways, thus changing the chemistry of the stream as shown by the hysteresis cycle. The counter-clockwise $^{87}Sr/^{86}Sr$ ratio-discharge for

Soapstone also suggests that stream chemistry during snowmelt is a result of change of water sources rather than a flush of solutes.

4.3 Propagation of event water downstream in nested catchment

The chemical signal at Soapstone (highest elevation stream sampling site) is propagated downstream through lower sites during the snowmelt season, suggesting that stream chemistry is controlled by processes at snowmelt sources. A two-component end-member mixing analysis utilizing Sr concentration and $^{87}Sr/^{86}Sr$ ratio was constructed for Woodland and Hailstone. The two end-members are the average Sr concentration and $^{87}Sr/^{86}Sr$ ratio Soapstone during the snowmelt. The other end-member is the average Sr concentration and $^{87}Sr/^{86}Sr$ ratio during base flow for that site (Fig. 5). Sr concentrations and $^{87}Sr/^{86}Sr$ ratios trend toward the Soapstone signature with a maximum contribution greater than 75% (Fig. 6). Concentration-discharge relationships at Woodland and Hailstone for DOC, Si and Pb also support that event water is propagated from through the stream system by concentrations trending toward Soapstone concentrations at peak discharge. In addition, $^{87}Sr/^{86}Sr$ ratio-discharge supports that event water chemistry is propagated downstream through the catchment (Fig 4). The $^{87}Sr/^{86}Sr$ ratio has a distinct pattern by year with the 2017 year having significantly different elevated $^{87}Sr/^{86}Sr$ ratio during snowmelt compared to previous years. This difference in $^{87}Sr/^{86}Sr$ ratio supports that lower elevation stream chemistry during snowmelt is controlled by high elevation processes. REE also show distinct concentration differences between the different water years.

The distinct $^{87}Sr/^{86}Sr$ ratio signatures at Woodland and Hailstone between years also suggests that climatic conditions can directly affect stream chemistry which is less evident at Soapstone. It may be important to do more nested catchment studies to see C-Q relationships in relationship to difference climate conditions for REE patterns to better understand how climate conditions affect the release of REE into stream systems.

5. Conclusions

Our research explores the hydrological processes during snowmelt in an alpine catchment. We assumed that Sr concentrations and $^{87}Sr/^{86}Sr$ ratios during snowmelt reflect travel pathways to the stream. Stream chemistry is primarily controlled by shallow and intermediate flowpaths. In addition, daily hysteresis cycles for DOC, Si and Pb during snowmelt suggest that stream chemistry is controlled by shallow and intermediate flowpaths. After peak discharge in the stream, Sr concentrations and $^{87}Sr/^{86}Sr$ ratios trend toward the intermediate flowpath way signature. This shift later in the snowmelt season maybe do to intermediate flowpaths having longer residence time, so water is sourced at the same time, but has an effect in the stream chemistry later in the snowmelt. The mixing model suggests that stream chemistry at the up-stream site (Soapstone) may entirely be explained by a mixture of base flow, shallow flowpath, and intermediate flowpath water. This suggests that original chemical precipitation signature is not connected to stream chemistry during snowmelt, and that stream chemistry in the watershed is dependent on processes after snowmelt at snowmelt locations. Dust deposition in the soil allowed for differentiation between shallow and intermediate path ways. Atmospheric dust has a significantly lower $^{87}Sr/^{86}Sr$ ratio compared to bed rock at the up-stream site (Soapstone). Mixing

models indicate that shallow flowpath ways reacting with the soil are most influential during the initial stages of snowmelt. This suggests that during the initial stages of snowmelt dust accumulation in soils plays a major contribution to stream water chemistry. Dust deposition may also contribute to negative water quality in alpine stream systems, resulting in elevated concentrations of heavy metals and REE.

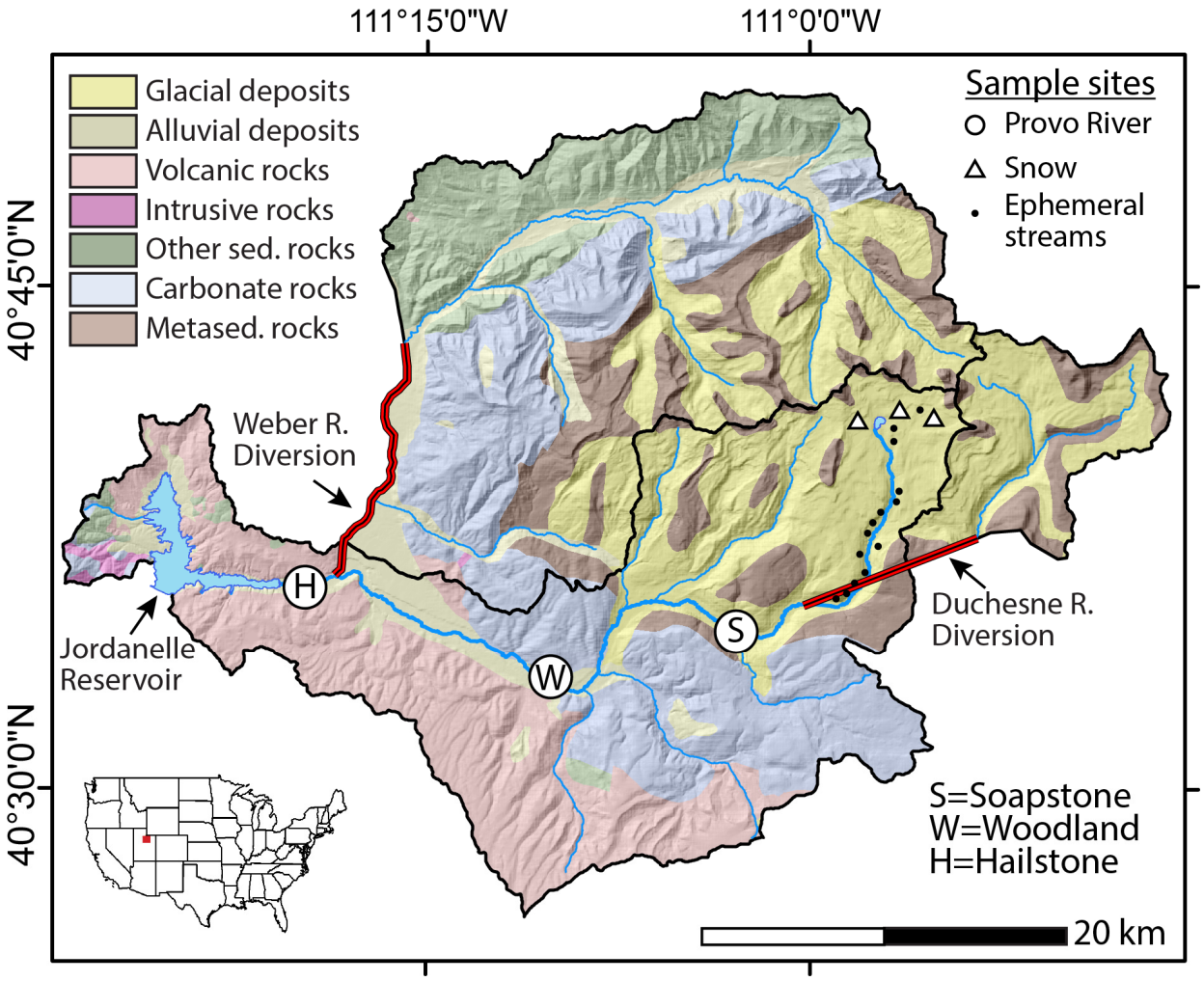

Figure 1. Simplified geologic and sample location map of the upper Provo River watershed including the Weber River diversion, and the Duchesne River diversion in northern Utah, USA.

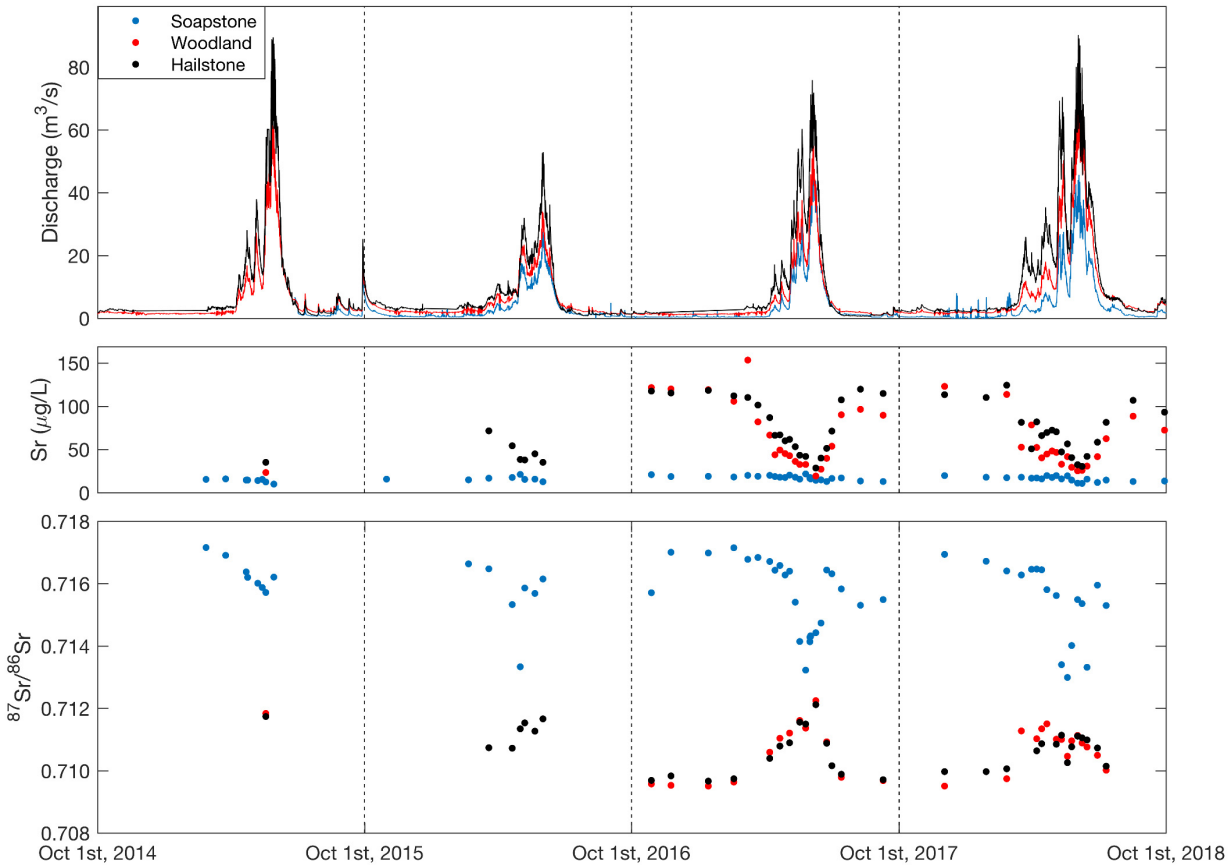

Figure 2. Stream discharge, Strontium (Sr) and $^{87}Sr/^{86}Sr$ ratios in the upper Provo River are seasonally and interannually variable. Sr concentrations at Soapstone are chemostatic while Woodland and Hailstone concentrations decrease by an order of magnitude during snow melt. The $^{87}Sr/^{86}Sr$ ratio at Soapstone, Woodland, and Hailstone during snow melt converge toward a $^{87}Sr/^{86}Sr$ ratio of 0.713 during snow melt.

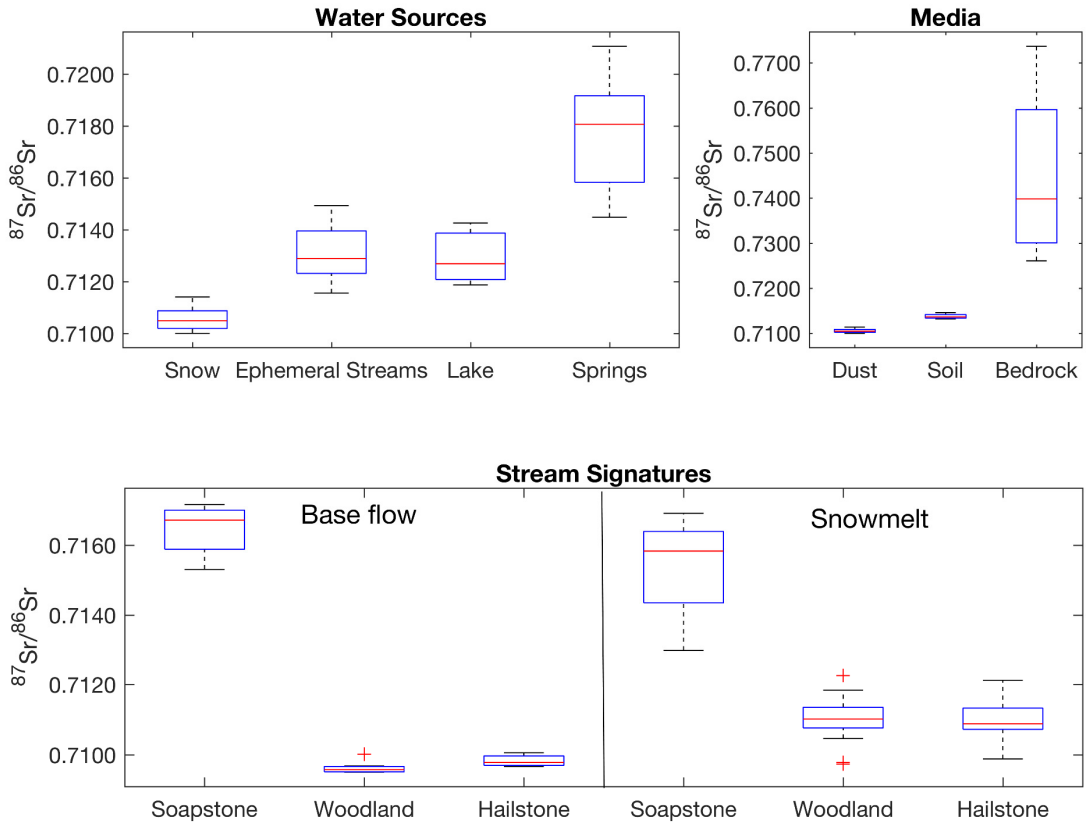

Figure 3. Top: Sources in the upper Provo River watershed display a large range of value from 0.7737 in bedrock to 07100 in dust. Bottom: $^{87}Sr/^{86}Sr$ ratio in the river samples show distinct ratios during high flow and low flow conditions at sampling sites. Bottom: A two-sample t-test between high flow and low flow at each site gives p-values of 0.005, 0.000002, and 0.000002 for Soapstone, Woodland, and Hailstone. Outline of box indicates 25th and 75th percentiles, and markers indicate maximum and minimum values. (Bedrock $^{87}Sr/^{86}Sr$ ratio obtain from Monroe, in prep.).

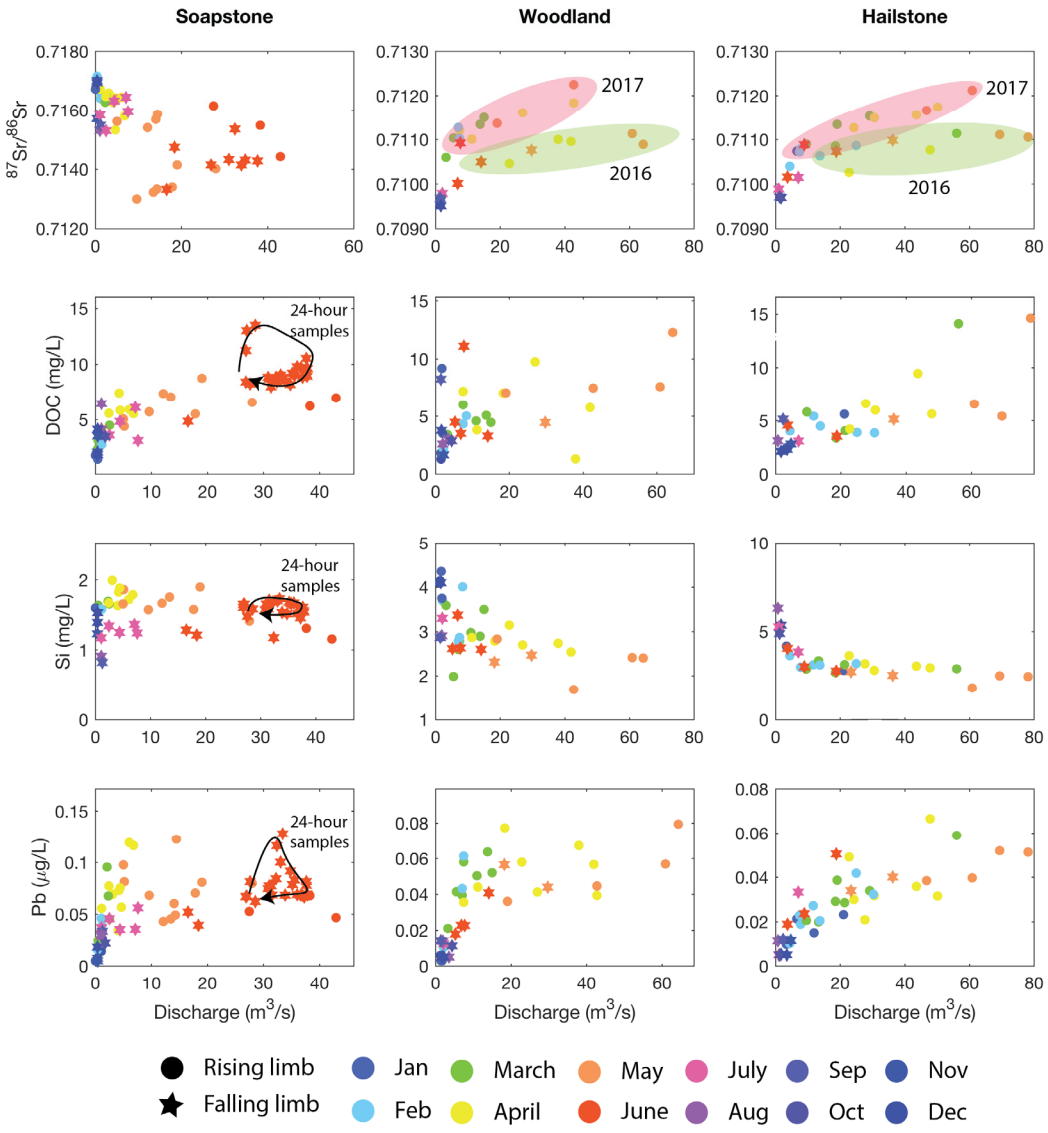

Figure 4. Concentration discharge plots for Soapstone, Woodland and Hailstone. The $^{87}Sr/^{86}Sr$ ratio during snow melt decreases at Soapstone but increases at Woodland and Hailstone. DOC, Si and Pb show clockwise hysteresis pattern during water year and 24-hours sampling event. The $^{87}Sr/^{86}Sr$ ratios show distinct signatures at Woodland and Hailstone for 2017, indicating that climate may affect water chemistry.

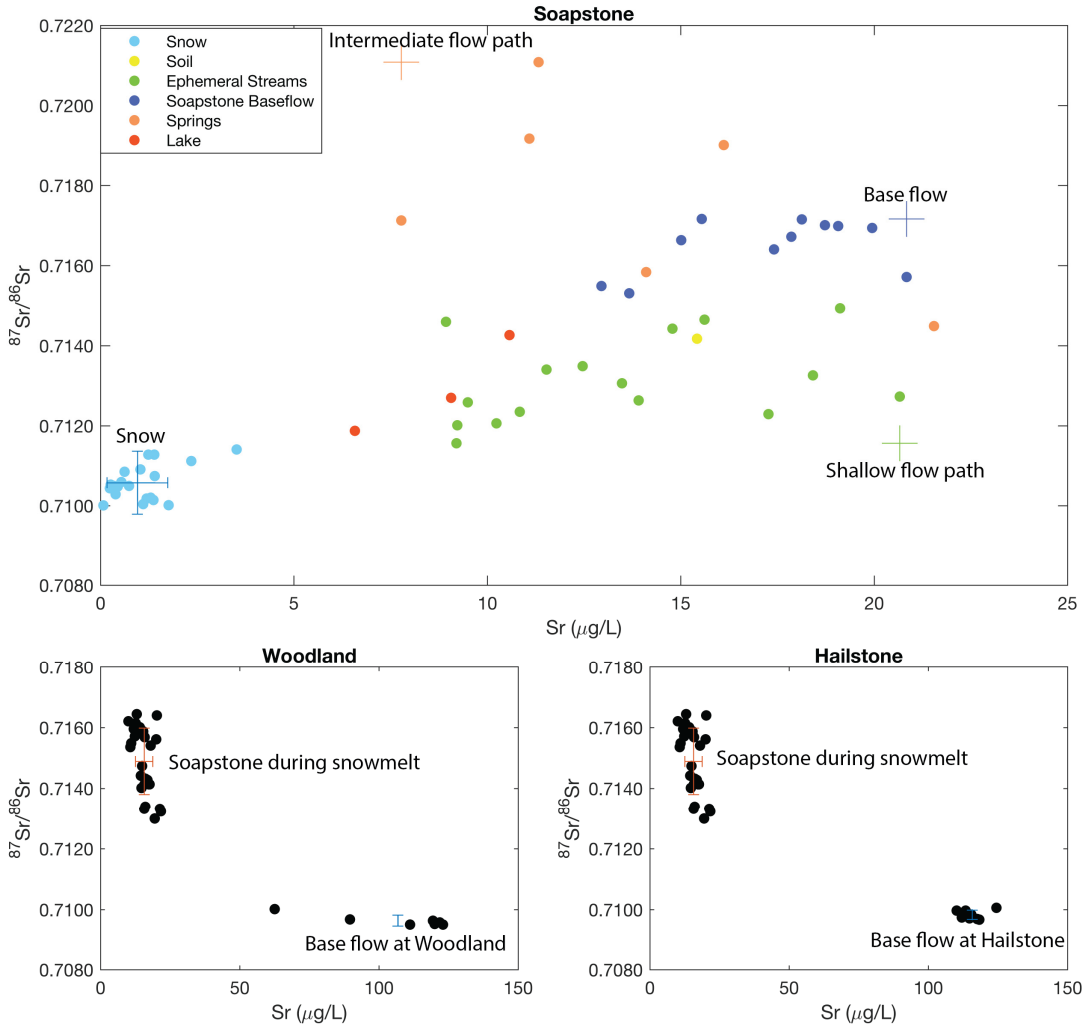

Figure 5. Soapstone plot indicates variance of Strontium (Sr) concentration and $^{87}Sr/^{86}Sr$ ratio for snow, soil, ephemeral Streams, springs, lakes and base flow at Soapstone. Crosses indicate chosen end-members for mixing analysis. The Snow end-member the average Sr concentration and $^{87}Sr/^{86}Sr$ ratio. Shallow flow path, intermediate flow path, and base flow end-members were chosen to be conservative. Shallow flow path end-member was chosen as the maximum Sr concentration and minimum $^{87}Sr/^{86}Sr$ ratio. Intermediate flow path endmember was chosen as the minimum Sr concentration, and the maximum $^{87}Sr/^{86}Sr$ ratio. Base flow end-member was chosen as the maximum Sr concentration and $^{87}Sr/^{86}Sr$ ratio. Upper end-member for Woodland and Hailstone mixing plots are the average Sr concentration and $^{87}Sr/^{86}Sr$ ratio for Soapstone during the months of May and June. Base flow endmember for Woodland and Hailstone plots are the average Sr concentration and $^{87}Sr/^{86}Sr$ ratio during September-February.

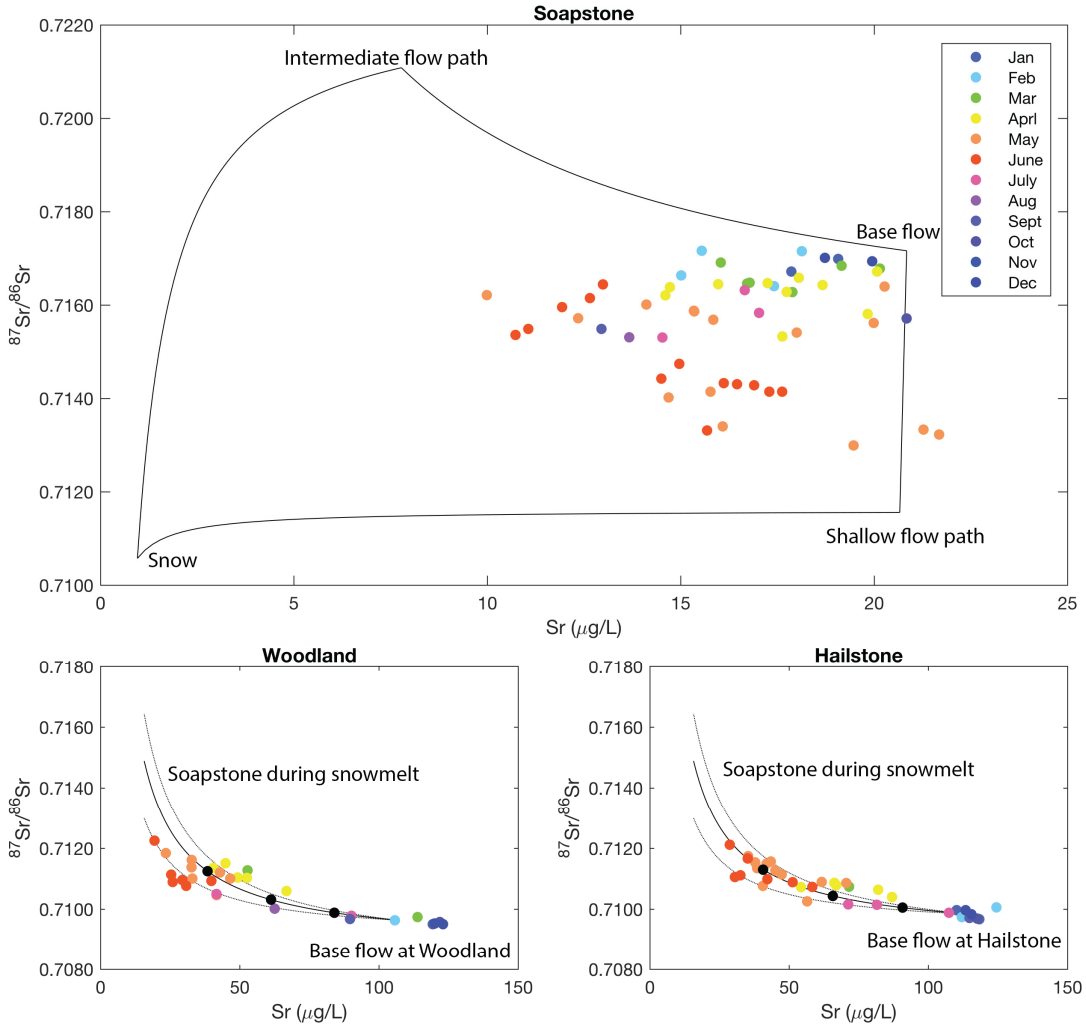

Figure 6. Strontium (Sr) concentration and $^{87}Sr/^{86}Sr$ ratio mixing plot for Soapstone, Woodland and Hailstone. Endmember choices based on figure 5. Soapstone plot shows stream water chemistry during peak run of trend toward ephemeral stream endmember. Post peak flow, stream chemistry shifts towards snow endmember. These shifts in stream water chemistry are interpreted as changes in dominant water sources from base flow, to shallow flow path, to intermediate flow path, then returning to base flow. Woodland and Hailstone mixing plots both show that downstream chemistry is dependent on upstream chemistry during snow melt.

6. References

Ågren, A., et al. (2010). "Regulation of stream water dissolved organic carbon (DOC) concentrations during snowmelt; the role of discharge, winter climate and memory effects." Biogeosciences 7(9): 2901-2913.

Ameli, A. A., et al. (2017). "Primary weathering rates, water transit times, and concentration-discharge relations: A theoretical analysis for the critical zone." WATER RESOURCES RESEARCH 53(1): 942-960.

Amundson, R., et al. (2007). "Coupling between Biota and Earth Materials in the Critical Zone." Elements 3: 327-332.

Andrews M. Grace, A. D. J., Gregory O. Lehn, and D. C. Travis W. Horton (2016). "Radiogenic and stable Sr isotope ratios (87Sr/86Sr, d88/86Sr) as tracers of riverine cation sources and biogeochemical cycling in the Milford Sound region of Fiordland, New Zealand." ScienceDirect 173: 284-303.

Bishop, K., Seibert Jan, Kojler Stephen, Laudon Hjalmar (2004). "Resolving the double Paradox of rapidly mobilized old water with highly variable responses in runoff chemistry." Hydrological processes 18: 185-189

Burns Douglas A., J. J. M., 1† Richard P. Hooper, Norman E. Peters, and C. K. James E. Freer, and Keith Beven (2001). "Quantifying contributions to storm runoff through end-member mixing analysis and hydrologic measurements at the Panola Mountain Research Watershed (Georgia, USA)." Hydrological processes(15): 1903-1924.

Burns M. A., H. R. B., R.S. Gabor, D.M. McKnight, and P. D. Broks (2016). "Dissolver organic matter transport reflects hillslope to stream connectivity during snowmelt in a montane catchment." Water Resour. Res. 52(4905-4923).

Carling, G. T., et al. (2012). "Dust-mediated loading of trace and major elements to Wasatch Mountain snowpack." Science of the Total Environment 432(0): 65-77.

Clark, I. a. F., Peter (1997). "Environmental Isotopes in Hydrogeology." CRC Press.

Clow David W. , M. W. W. b., Paul F. Schuster c and a. Colorado (2016). "Increasing aeolian dust doposition to snowpacks in the Rocky Mountains inferred from snowpack, wet deposition, and aerosol chemistry." Atmospheric Environment(146): 183-194.

Creed, I. F., et al. (2015). "The river as a chemostat: fresh perspectives on dissolved organic matter flowing down the river continuum." Canadian Journal of Fisheries and Aquatic Sciences 72(8): 1272-1285.

Foks Sydney S., E. G. S., Kamini Singha, David W. Clow, and a. W. Mission (2018). "Influence of climate on alpine stream chemistry and water sources." Hydrological processes.

Frisbee, M. D., et al. (2012). "Unraveling the mysteries of the large watershed black box: Implications for the streamflow response to climate and landscape perturbations." Geophysical Research Letters 39(1): n/a-n/a.

Godsey, S. E., et al. (2009). "Concentration-discharge relationships reflect chemostatic characteristics of US catchments." Hydrological processes 23(13): 1844-1864.

James F. Hogan James F., a. J. D. B. (2003). "Tracing hydrologic flow paths in a small forested watershed using variations in 87Sr//86Sr, [Ca]//[Sr], [Ba]//[Sr] and D18O." WATER RESOURCES RESEARCH 39(10): 1282.
Kim, H., et al. (2012). "Autonomous water sampling for long-term monitoring of trace metals in remote environments." Environ Sci Technol 46(20): 11220-11226.
Kim, H., et al. (2017). "Controls on solute concentration-discharge relationships revealed by simultaneous hydrochemistry observations of hillslope runoff and stream flow: The importance of critical zone structure." WATER RESOURCES RESEARCH 53(2): 1424-1443.
Kirchner, J. W. (2003). "A double paradox in catchment hydrology and geochemistry." Hydrological processes 17(4): 871-874.
Kirchner, J. W. (2006). "Getting the right answers for the right reasons: Linking measurements, analyses, and models to advance the science of hydrology." WATER RESOURCES RESEARCH 42(3).
Kirchner, J. W. (2009). "Catchments as simple dynamical systems: Catchment characterization, rainfall-runoff modeling, and doing hydrology backward." WATER RESOURCES RESEARCH 45(2).
Kirchner, J. W., et al. (2000). "Fractal stream chemistry and its implications for contaminant transport in catchments." Nature 403.
Liu Fengjing, M. W. W., and Nel Caine (2004). "Source waters and flow paths in an alpine catchment, Colorado Front Range, United States." Water Resour. Res. 40.
Liu, F., et al. (2008). "Seasonal and interannual variation of streamflow pathways and biogeochemical implications in semi-arid, forested catchments in Valles Caldera, New Mexico." Ecohydrology 1(3): 239-252.
Lowry, G. V., et al. (2004). "Macroscopic and microscopic observations of particle-facilitated mercury transport from New Idria and Sulphur Bank mercury mine tailings." Environmental Science and Technology 38(19): 5101-5111.
McNamara, J. P., et al. (2011). "Storage as a Metric of Catchment Comparison." Hydrological processes 25(21): 3364-3371.
Miller, O. L., et al. (2014). "Evaluating the use of strontium isotopes in tree rings to record the isotopic signal of dust deposited on the Wasatch Mountains." Applied Geochemistry 50(0): 53-65.
Munroe, inprep. Personal communication.
Neal, C., et al. (2013). "High-frequency precipitation and stream water quality time series from Plynlimon, Wales: an openly accessible data resource spanning the periodic table." Hydrological processes 27(17): 2531-2539.
Neff, J. C., et al. (2008). "Increasing eolian dust deposition in the western United States linked to human activity." Nature Geoscience 1(3): 189-195.
Reynolds Richard, J. B., Marith Reheis, Paul Lamothe, and Fred Luiszer (2001). "Aeolian dust in Colorado Plateau soils: Nutrient inputs and recent change in source." PNAS 98(13): 7123-7127.

Reynolds, R. L., et al. (2010). "Compositional changes in sediments of subalpine lakes, Uinta Mountains (Utah): evidence for the effects of human activity on atmospheric dust inputs." Journal of Paleolimnology 44(1): 161-175.
Vázquez-Ortega, A., et al. (2015). "Rare earth elements as reactive tracers of biogeochemical weathering in forested rhyolitic terrain." Chemical Geology 391: 19-32.
Steiger, R. H. and E. Jäger (1977). "Subcommission on geochronology: Convention on the use of decay constants in geo- and cosmochronology." Earth and Planetary Science Letters 36(3): 359-362.
USEPA. Method 1669: Sampling Ambient Water for Trace Metals at EPA Water Quality Criteria Levels : Draft: U.S. Environmental Protection Agency, Office of Water, 1996.
USEPA. Mercury Study Report to Congress. In: Agency USEP, editor. EPA-452-97-003. Office of Air and Radiation, Washington, D.C., 1997.
USEPA. EPA Method 1631, Revision E: Mercury in Water by Oxidation , Purge and Trap, and Cold Vapor Atomic Fluorescence. Revision E. US Environmental Protection Agency, Washinton D.C., 2002, pp. 38 pp.